

Investigation of RPV samples of the Greifswald NPP with focus on retrospective dosimetry

Erik Poenitz^{1,*} and Joerg Konheiser¹

¹Helmholtz-Zentrum Dresden-Rossendorf, Bautzner Landstraße 400, 01328 Dresden, Germany

Abstract. Reactor pressure vessel (RPV) samples of units 1 and 4 of the Greifswald NPP were investigated with focus on retrospective dosimetry. Specific activities of long-lived radionuclides ^{63}Ni , $^{93\text{m}}\text{Nb}$, ^{94}Nb and ^{99}Tc as well as the concentrations of the producing elements were measured. Investigated samples comprise base metal, welding metal and cladding of the RPV. Neutron fluences obtained with the Monte-Carlo codes TRAMO and MCNP were used to calculate specific activities. The gamma-emitter ^{94}Nb appears as a promising candidate due to the large Nb concentration in the cladding of the VVER RPs. For $^{93\text{m}}\text{Nb}$, a very good agreement of measured and calculated activities was found for the RPV cladding samples where $^{93\text{m}}\text{Nb}$ is primarily produced by the threshold reaction $^{93}\text{Nb}(n,n')^{93\text{m}}\text{Nb}$. A strong scatter of the ratios of calculated and experimental activities is observed for ^{63}Ni which is primarily produced by slow neutrons. For ^{99}Tc , a good agreement of calculated and measured activities was found for the majority of the base metal and welding metal samples but not for the cladding samples. Updated reaction cross section data for $^{62}\text{Ni}(n,\gamma)$ and $^{92}\text{Mo}(n,\gamma)$ lead to a better agreement of calculated and measured activities for ^{63}Ni and $^{93\text{m}}\text{Nb}$.

1 Introduction

The units 1 to 4 of the Greifswald Nuclear Power Plant (NPP) started operation in the 1970s and were shut down in 1990 during the German reunification. In the years after the shutdown, reactor pressure vessel (RPV) trepanns of units 1, 2 and 4 were taken which provide excellent opportunities for the investigation of irradiated VVER-440 RPV materials. An overview of earlier investigations of the Greifswald NPP trepanns can be found in [1].

The surveillance of the radiation embrittlement of the RPV caused by neutron irradiation has a high priority. For the VVER-440/230, no surveillance specimen programme existed. For subsequent generations of VVER, surveillance programmes were implemented. However, technical issues of the standard surveillance programme of the VVER-440/213 are discussed in [2]. The measurement of long-lived radionuclides in samples taken from the inner wall or outer wall of the RPV can provide an (additional) experimental validation for the calculation of the neutron fluences if no or insufficient surveillance specimen data are available.

* Corresponding author: e.poenitz@hzdr.de

Samples of RPV trepans of units 1 and 4 of the Greifswald NPP were investigated with focus on retrospective dosimetry. Specific activities of long-lived radionuclides ^{63}Ni , $^{93\text{m}}\text{Nb}$, ^{94}Nb and ^{99}Tc as well as the elemental compositions were measured. Investigated samples comprise base metal, welding metal and cladding of the RPV. Calculations of specific activities and neutron fluences were carried out using the Monte-Carlo codes TRAMO [3] and MCNP [4].

2 Activity measurement and calculation

2.1 RPV samples

Mass fraction and activity measurements were carried out for 14 samples of RPV trepans of units 1 and 4 of the Greifswald NPP. Samples were taken from nine positions. In some positions, two samples were measured to check the reproducibility of the measurements.

For unit 1, the sample positions cover the circumferential welding seam adjacent to the reactor core and the base metal of two different heights. In contrast to unit 1, the inner wall of the RPV of unit 4 is completely cladded. For unit 4, the sample positions cover the cladding and the base metal. Details of the sample positions are given in Table 1.

Table 1. Sample designation, material, position and calculated fast neutron fluence of the investigated samples. The height refers to the lower edge of the fission zone.

| Sample designation (Unit-trepan number.disc) | Material | Height in cm | Angle | Depth in mm | $\Phi(E_n > 0.5 \text{ MeV})$ in 10^{19} cm^{-2} | |
|--|--------------------------------|-----------------|-------|----------------|---|-------|
| | | | | | TRAMO | MCNP |
| 1-1.1 | Welding seam | 30 | 330° | 3 – 13 | 3.909 | 4.238 |
| 1-1.17 | | | | 126 – 136 | 1.159 | 1.218 |
| 1-4.1 | Base metal | 72 | 330° | 3 – 13 | 5.163 | 5.750 |
| 1-4.16 | | | | 127 – 137 | 1.564 | 1.651 |
| 1-3i | Base metal (low irradiated) | 275 | 300° | 0 – 2 | 0.148 | 0.113 |
| 1-3o | | | | 138 – 140 | 0.085 | 0.084 |
| 4-1.1 | Cladding | 110 | 30° | 4 – 5.3 | 5.373 | 6.299 |
| 4-1.8 | Base metal | | | 69 – 79 | 3.172 | 3.577 |
| 4-1.16 | | | | 136 – 146 | 1.467 | 1.653 |

Most of the samples are taken from broken Charpy-V specimen. For the cladding samples, a 1.3 mm thick plate was cut from the side directed to the RPV inner wall to ensure that the plate consists solely of the Nb-containing 2nd layer of the cladding. Trepan 1-3 was not yet cut into discs to produce Charpy-V specimen. Here, 2 mm thick plates were cut from the inner-wall and outer-wall side of the trepan and designated 1-3i and 1-3o, respectively. The depth refers to the surface between downcomer and RPV steel for unit 1. For unit 4, it refers to the surface between downcomer and cladding.

2.2 Mass fraction and activity measurements

The mass fraction and activity measurements were carried out at the accredited laboratory for environmental and radionuclide analysis of VKTA – Strahlenschutz, Entsorgung und Analytik Rossendorf e.V. Mass fractions were measured by Inductively-Coupled Plasma Mass-Spectrometry (ICP MS) for the elements Ni, Cu, Nb and Mo. After radiochemical separation of the corresponding elements, the specific activities of ^{63}Ni and $^{93\text{m}}\text{Nb}$ were

measured by Liquid Scintillation Counting (LSC) and the ones of ^{99}Tc by ICP MS. A detailed description of the analytics is given in [5].

Additionally, the specific activity of ^{94}Nb was measured by gamma spectrometry for the two cladding samples with a Nb mass fraction of approx. 0.7 %. The measurement of the ^{94}Nb activity of the other twelve samples was not possible due to the small Nb mass fraction of approx. 1 ppm. Even after a decay time of nearly three decades since the shutdown of the NPPs, the ^{60}Co activity of the base metal and welding seam samples is approx. 5 orders of magnitude larger than the one of ^{94}Nb .

2.3 Calculation of specific activities

The Monte-Carlo radiation transport codes TRAMO [3] and MCNP [4] were used for the calculation of spectral neutron fluences. TRAMO is developed by HZDR and is primarily employed for reactor dosimetry. MCNP is a general-purpose Monte-Carlo code which is widely used as a reference code for radiation transport calculations. Care was taken to ensure that identical data for the geometry model (measures, material compositions) were used in the geometry models of the codes. The focus of the article is the MCNP calculations. The TRAMO calculations provide comparative values to verify the newly developed MCNP-model. The neutron source and its distributions were generated on the basis of data calculated using a standard burnup program. The data were already provided by NIS Ingenieursgesellschaft mbH Rheinsberg (now: Siempelkamp NIS) for an earlier investigation program [5].

The MCNP geometry model covers the complete RPV including reactor internals, reactor lid and the complete annular water tank. Cross sections and fission spectra are taken from the library ENDF/B-VIII.0 [6]. Individual calculations were carried out for each cycle to account for changes in the geometry model, i.e. average boron concentration and loading schemes. Additional simulations were done to investigate the influence of the change of the boron concentration during the cycle.

Spectral neutron fluences at the position of the samples were calculated using the track-length estimator tally. A logarithmically equidistant group structure with 60 groups per energy decade (679 groups from 10^{-10} MeV to 20 MeV) was chosen. Compared to the SAND-II-A group structure widely used in reactor dosimetry (640 groups from 10^{-10} MeV to 20 MeV), it provides a better resolution in both the thermal neutron and resonance region. For the calculation of the reaction rates, reaction cross sections were primarily taken from the library ENDF/B-VIII.0. For the reaction $^{93}\text{Nb}(n,n')^{93\text{m}}\text{Nb}$, cross sections of the library IRDFF-II [7] are favoured. Reaction cross sections not available in the library ENDF/B-VIII.0 were taken from JEFF 3.0A [8]. Specific activities were calculated with a numerical code.

3 Results

3.1 Neutron fluence spectra

Neutron fluence spectra (MCNP calculation) of the samples 4.1-1, 4.1-8 and 4.1-16 taken from unit 4 of the Greifswald NPP are shown in Figure 1. Compared to the outer-wall sample (lower curve), the neutron fluence for neutron energies above 0.5 MeV is 4 times as large for the sample taken from the inner wall (upper curve) in good agreement with earlier calculations [1].

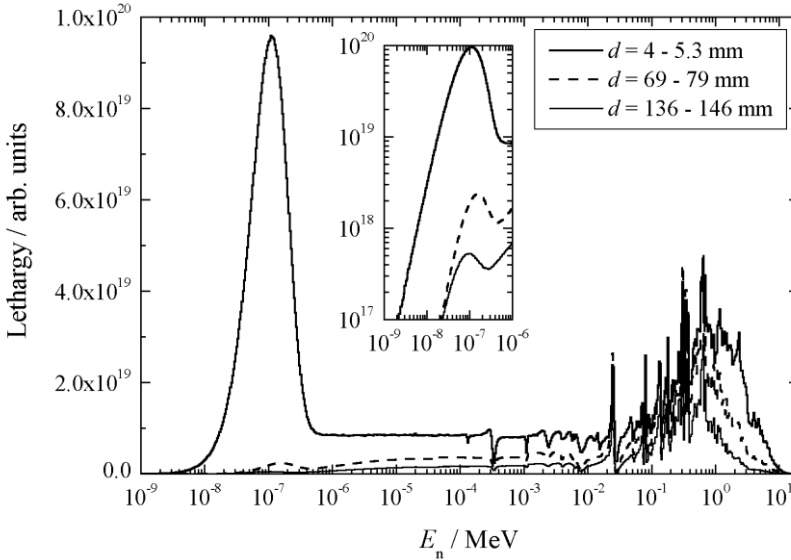


Fig. 1. Spectral neutron fluences at the positions of the samples taken from the inner wall (upper curve), centre of the RPV (middle curve) and outer wall (lower curve) of unit 4 of the Greifswald NPP. The thermal neutron peaks are shown with a logarithmic scale in the inset.

With the exception of ^{93m}Nb in the cladding, the radionuclides of interest are primarily produced by slow and epithermal neutrons. The neutron spectrum for the inner-wall sample has a large contribution of thermal neutrons which strongly depends on the boron concentration in the coolant water. This is especially important for ^{63}Ni which is primarily produced by thermal neutrons due to the large thermal cross section compared to the resonance integral of the $^{62}\text{Ni}(n,\gamma)$ reaction. The part of the slow neutrons in the neutron spectra for the centre of the RPV (middle curve) and for the outer wall are much smaller due to the absorption in the RPV steel. As can be seen in the inset of Figure 1, the thermal peak of the neutron spectrum of the centre of the RPV shows a hardening, i.e. a small shift to higher energies. The neutron spectrum for the sample taken from the outer wall, however, shows a shift of the thermal peak to lower energies. Essentially all thermal neutrons and a large part of the epithermal neutrons are backscattered by the annular water tank as can be shown using MCNP's cell-flagging capability. The water temperature in the annular water tank (approx. 60°C) is much lower than the one in the downcomer region (265°C).

3.2 Mass-specific activities

Measured and calculated specific activities for the nuclides ^{93m}Nb , ^{94}Nb , ^{63}Ni and ^{99}Tc are shown in Figures 2 to 5. As can be seen for the samples taken from trepans 1-1 and 1-4, the specific activity of ^{63}Ni is larger for the inner wall samples than for the outer wall samples by a factor of approx. 60. Even for the nuclides ^{93m}Nb and ^{99}Tc which are primarily produced by neutrons in the resonance region, the activity ratio is somewhat larger than the ratio of the fast neutron fluences shown in Table 1. Trepan 1-3 was taken from a position above the reactor core. The specific activities as well as the fast neutron fluences shown in Table 1 are much smaller. The ratios of both fast neutron fluences and activities for the inner-wall and outer-wall samples are much smaller than for the samples in height of the

reactor core. This is attributed to neutron streaming via the gap between RPV and thermal insulation/annular water tank. Compared to samples from the inner wall of the RPV of unit 1, the specific activities of ^{93m}Nb , ^{94}Nb and ^{63}Ni of the samples 4-1.1 (cladding) are especially large. It is caused to the large mass fractions of Ni (10 %) and Nb (0.7 %) in the Nb-stabilized austenitic steel. The small Mo mass fraction in the cladding leads to comparatively small ^{99}Tc activities of the samples 4-1.1. Both TRAMO and MCNP calculations have a tendency to underestimate the measured specific activities.

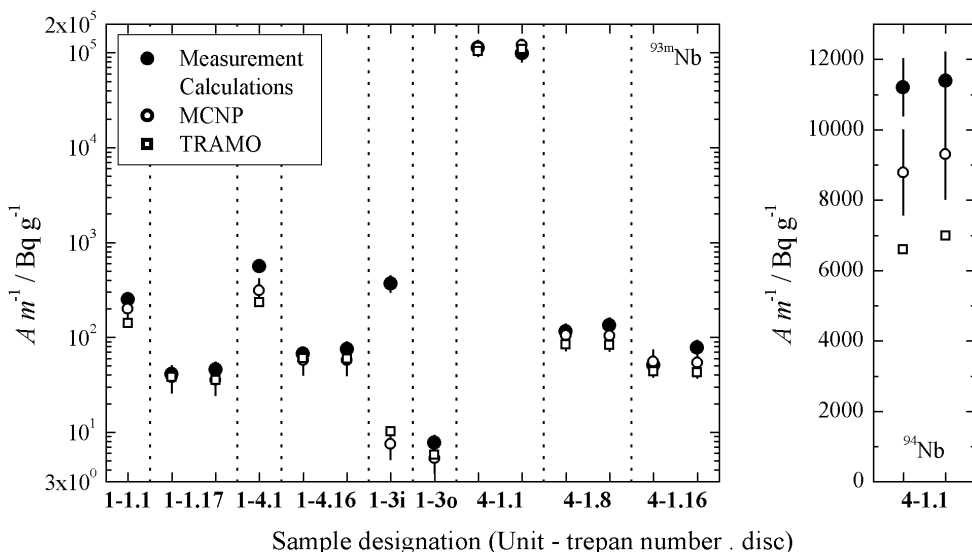


Fig. 2. Measured and calculated specific activities for ^{93m}Nb (left) and ^{94}Nb (right). Due to the small Nb mass fraction in the base metal and welding seam samples, ^{94}Nb specific activity measurements are available only for the cladding samples.

Specific activities of ^{93m}Nb are shown in Figure 2 (left). In the two cladding samples with measured Nb mass fractions of 6800 ppm and 7200 ppm, ^{93m}Nb ($T_{1/2} = 16.12 \text{ y}$) is almost exclusively produced by the threshold reaction $^{93}\text{Nb}(n,n^{\prime})$ widely used in reactor dosimetry of ex-vessel activation detectors. For both measurements, a good agreement of measured and calculated activities was found (ratio of calculated and experimental activities $C_{\text{TRAMO}}/E = 0.91$ and 1.10 , $C_{\text{MCNP}}/E = 1.01$ and 1.22 , respectively). Because of the alloying element molybdenum in the base metal and welding seam samples, ^{93m}Nb is primarily produced by the reaction $^{92}\text{Mo}(n,\gamma)^{93}\text{Mo}$ and the subsequent decay of ^{93}Mo to ^{93m}Nb . Here, niobium is only a trace element with a mass fraction of ca. 1 ppm. While large, the half-life time ($T_{1/2} = 4000 \text{ y} \pm 800 \text{ y}$) of ^{93}Mo and the branching ratio ($88 \% \pm 12 \%$) for the decay into ^{93m}Nb are not well-known leading to large uncertainties of the calculated specific activities.

A new evaluation of the $^{92}\text{Mo}(n,\gamma)$ reaction cross section is available in the library ENDF/B-VII.1 [9]. The cross section is larger by a factor of 4 in the $1/v$ region and remains essentially unchanged in the resonance region. Applying the new evaluation greatly improves the agreement of calculated and experimental ^{93m}Nb activities of the base metal and welding seam samples taken from the inner wall of the RPV without changing the good agreement for the outer-wall samples.

Specific activities for ^{94}Nb ($T_{1/2} = 20\,300 \text{ y} \pm 1\,600 \text{ y}$) are shown in Figure 2 (right). Experimental data are only available for the cladding samples 4-1.1.

In the libraries ENDF/B-VIII.0 and IRDFF-II, new evaluations of the $^{93}\text{Nb}(n,\gamma)^{94}\text{Nb}$ reaction cross section are available and lead to approx. 5 % smaller calculated activities of the cladding samples compared to the evaluations in the old libraries ENDF/B-VII.0 [10] and IRDF-2002 [7]. In the right panel of Figure 2, activities calculated with the newly evaluated reaction cross section are shown.

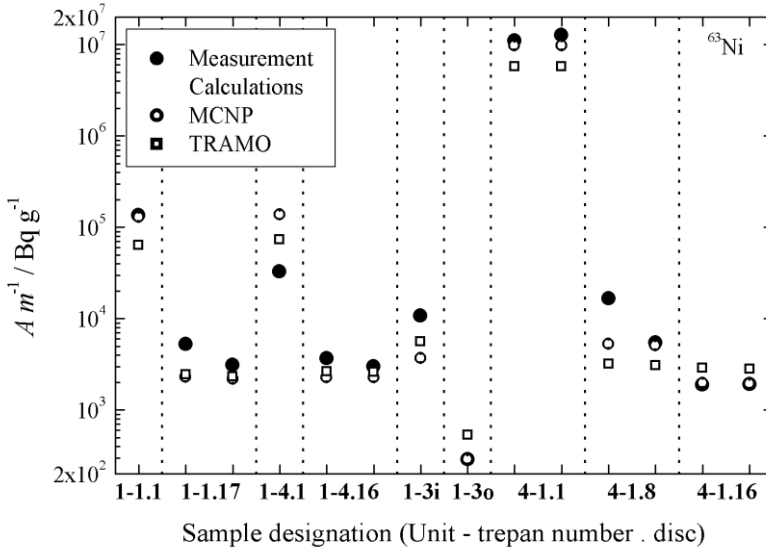


Fig. 3. As Fig. 2 but for $^{59+63}\text{Ni}$.

Measured and calculated specific activities for ^{63}Ni ($T_{1/2} = 101.2$ y) are shown in Figure 3. It is primarily produced by the reaction $^{62}\text{Ni}(n,\gamma)$. The contribution by the $^{63}\text{Cu}(n,p)$ reaction is very small for most of the samples but can amount for approx. 10 % of the ^{63}Ni activity for some outer-wall samples with small Ni and large Cu mass fractions. It is assumed that the ^{59}Ni ($T_{1/2} = 76\ 000$ y) decay cannot be separated from ^{63}Ni decay in LSC measurements. Therefore, the sum of calculated specific activities of ^{59}Ni and ^{63}Ni is shown in Figure 3. However, due to the large half-life time, the isotopic ratio of $^{58}\text{Ni}/^{62}\text{Ni}$ and the (n,γ) cross section ratio, it is expected that the ^{59}Ni activity is only 1 % of the ^{63}Ni activity.

In the library ENDF/B-VII.1, new evaluations of the reaction cross sections for $^{58}\text{Ni}(n,\gamma)$ and $^{62}\text{Ni}(n,\gamma)$ are available. Compared with the library ENDF/B-VII.0, the $^{62}\text{Ni}(n,\gamma)^{63}\text{Ni}$ cross section is 3.4 % larger (thermal neutrons) and 22 % larger (resonance integral). The activities calculated with the new evaluation are approx. 4 % (inner wall) to 12 % (outer wall) larger and show a better agreement with measured activities for nearly all samples. The change of the $^{58}\text{Ni}(n,\gamma)$ reaction cross section has only a small influence on the calculated activities shown in Figure 3 due to the small contribution of the ^{59}Ni activity.

The specific activities of ^{99}Tc ($T_{1/2} = 211\ 100$ y) are shown in Figure 4. A rather good agreement of calculated and measured activities is observed for the majority of the base metal and welding seam samples but not for the cladding samples (4-1.1). As larger Mo mass fractions were measured for cladding samples in earlier investigations, possible reasons are an inhomogeneous distribution of Mo in the cladding or problems with the Mo mass fraction measurements. Additionally, a not satisfactory separation of ^{93m}Nb was observed in [5].

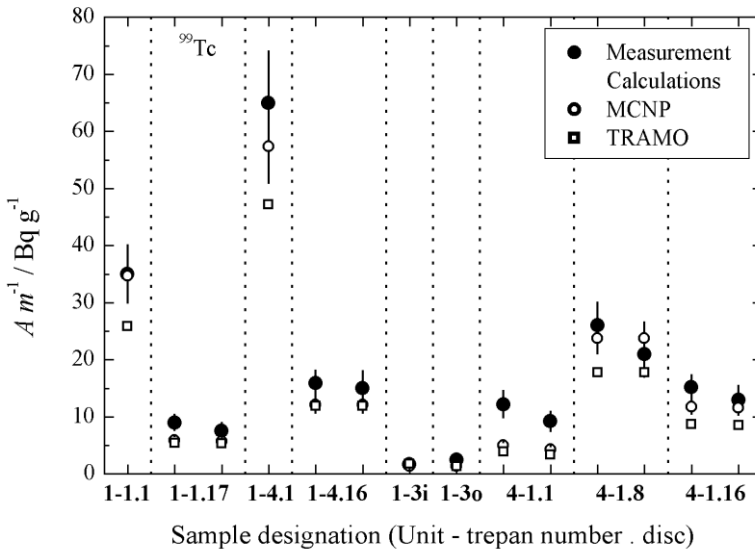


Fig. 4. As Fig. 2 but for ⁹⁹Tc.

4 Conclusions

Specific activities were measured and calculated for long-lived radionuclides ⁶³Ni, ^{93m}Nb, ⁹⁴Nb and ⁹⁹Tc which might be of interest for retrospective dosimetry. Both calculation and measurement are more challenging compared with the mostly threshold-reaction ex-vessel activation detectors. This is indicated by larger uncertainties and a stronger scatter of the ratios of calculated and experimental activities *C/E*.

For ^{93m}Nb, a good agreement of calculated and measured activities was found for the majority of the samples. In the cladding samples, ^{93m}Nb is primarily produced by the threshold reaction ⁹³Nb(n,n') widely used in reactor dosimetry. The uncertainty of the activity measurements, however, is rather large and leads to uncertainties of the *C/E* ratio of 22%. For the base metal and welding seam samples, the uncertainties of the *C/E* ratio are even larger (35%) due to the large uncertainties of the ⁹³Mo half-life time and branching ratio.

The radionuclide ⁹⁴Nb appears as a promising candidate. In contrast to the other long-lived nuclides, it emits hard gamma radiation and can be measured by gamma spectrometry without Nb separation. The uncertainty of the *C/E* ratio is comparatively small (15%). Due to the very small Nb mass fractions in the VVER RPV steel and the welding material, the measurement is limited to the 2nd layer of the cladding of VVER RPV which consists of an Nb-stabilized austenitic steel. If Nb-containing steel like AISI 347 can be investigated, the retrospective dosimetry of ⁹⁴Nb might also be of interest for other types of NPPs.

The activity measurements were carried out in April 2018, i.e. nearly 3 decades after the shutdown of the NPP. The ratio of the specific activities of ⁶⁰Co and ⁹⁴Nb in the cladding was approx. 60 at the date of the measurement. For samples taken from a NPP in the operation phase, a larger activity ratio of approx. 1000 has to be expected. A ⁹⁴Nb activity measurement by gamma spectrometry without separation of other gamma-emitting radionuclides is expected to be possible but will require long measurement times of at least 12 h to 24 h.

The radionuclide ^{63}Ni was expected to be very convenient for retrospective dosimetry because of its half-life of 100 years. Additionally, the specific activities of all samples are comparatively large and therefore less sensitive to an incomplete separation of other radionuclides. However, even if one excludes two outliers, the C/E ratios show a very strong scatter and do not provide a reliable validation for the calculation of fast neutron fluences.

The radionuclide ^{99}Tc shows both advantages and disadvantages. With the exception of one outlier, the calculated and measured activities are in a good agreement for base metal and welding seam samples. Due to the comparatively large resonance integral of the $^{98}\text{Mo}(n,\gamma)$ reaction, thermal neutrons have a rather small influence on the ^{99}Tc production. Due to the very large half-life time and the corresponding small activity, the activity measurement requires high demands on the separation of other radionuclides. For cladding samples of VVER RPV, the application of ^{99}Tc for retrospective dosimetry appears disfavoured.

This work was funded by the German Ministry of Economic Affairs and Energy (Grant-No. 1501531 – mass fraction and activity measurements) and by the German Ministry of Education and Research (Grant-No. 015S9412 – radiation transport calculations).

References

1. H.-W. Viehrig et al., report HZDR-Bericht 88 (2018), ISSN 2191-8708, eISSN 2191-8716
2. M. Brumovský et al., IAEA-TECDOC-1442 (2005), ISBN 92-0-105605-2
3. H.-U. Barz, J. Konheiser, report FZR Bericht-245 (1998)
4. C. J. Werner (editor), MCNP® User's Manual, Code Version 6.2 (2017), LA-UR-17-29981
5. J. Konheiser et al., J.ASTM Intl. **9(3)** (2012), doi: 10.1520/JAI103925 (2012)
6. D.A. Brown et al., Nuclear Data Sheets **148** 1-142 (2018)
7. A. Trkov et al., IRDFF-II: A New Neutron Metrology Library (2019), arXiv:1909.03336v2[nucl-th]21 Oct 2019
8. J.-Ch. Sublet et al., Proceedings of the Int. Conf. on Nuclear Data for Science and Technology 203 (2005), doi: 10.1063/1.1944990
9. M.B. Chadwick et al., Nuclear Data Sheets **112** 2887-2996 (2011)
10. M.B. Chadwick et al., Nuclear Data Sheets **107** 2931-3060 (2006)